available at http://ajws.elsevier.com/tcmj

Tzu Chi Medical Journal

Review Article

Clinical Applications and Usefulness of Integrated Single Photon Emission Computed Tomography/ Computed Tomography Imaging

Pan-Fu Kao[1,2], Yu-Hsiang Chou[1]*

[1]*Department of Nuclear Medicine, Buddhist Tzu Chi General Hospital, Taipei Branch, Taipei, Taiwan*
[2]*Department of Radiological Technology, Tzu Chi College of Technology, Hualien, Taiwan*

Article info

Article history:
Received: March 31, 2008
Revised: April 14, 2008
Accepted: May 1, 2008

Keywords:
Bone scan
^{67}Ga inflammation scan
Parathyroid scan
Sentinel lymph node
Single photon emission computed tomography/ computed tomography (SPECT/CT)
Thyroid cancer survey

Abstract

Radiopharmaceuticals reflect physiologic and pathologic functions rather than anatomical abnormalities. In the clinical setting, it is often necessary to correlate these functional studies using anatomical imaging. The advent of single photon emission computed tomography (SPECT) and positron emission tomography (PET) provides tomographic images for direct correlation to anatomic modalities such as X-ray, computed tomography (CT) and magnetic resonance imaging. Correlation of anatomic and functional information can aid in the decision-making process by enabling better localization and definition of organs and lesions and improving the precision of surgical biopsies. The advantages of combining SPECT with CT are primarily due to the anatomical referencing and the attenuation correction capabilities of CT. Depending on the system design, there are varying technical issues surrounding the different SPECT/CT devices. The principle of the integrated SPECT/CT instrumentation and the use of attenuation correction and anatomical referencing are discussed in this review. The specific disease processes where SPECT/CT has had a positive impact on diagnostic accuracy will be illustrated in this review. Although it is starting more slowly than PET/CT, SPECT/CT has many existing and potential areas of clinical application and has significantly added to the diagnostic power of nuclear medicine. Through literature review and case presentation, the authors illustrate the applications and uses of SPECT/CT as experienced at Tzu Chi General Hospital. The most common uses of SPECT/CT were for the diagnoses of infections focused with gallium-67 citrate, ^{99m}Tc-sulfur-colloid sentinel lymph node mapping, thyroid cancer survey with ^{131}I-sodium iodide, parathyroid scan with ^{99m}Tc-Sestamibi, abdominal diseases, and bone imaging with ^{99m}Tc-methylene diphosphonate. Through this review, the authors also highlight the current comprehensive clinical use of SPECT/CT in our hospital. (*Tzu Chi Med J* 2008;20(4):253–269)

*Corresponding author. Department of Nuclear Medicine, Buddhist Tzu Chi General Hospital, Taipei Branch, 289, Jianguo Road, Xindian City, Taipei, Taiwan.
E-mail address: pfkao@yahoo.com.tw

1. Introduction

During the past 10 years, there has been growing utilization of positron emission tomography (PET) due to health care insurance reimbursement for cancer staging and therapy response evaluation [1]. A great deal of the use of PET scans has also been stimulated by its co-registration with computed tomography (CT) acquired during the same patient visit. These PET/CT fusion studies produce functional and anatomic correlative images that may add greater specificity and sensitivity than previously available from radionuclide studies alone [1].

The traditional nuclear medicine procedures with single-photon tracers still constitute the majority of clinical services. In recent years, single photon emission computed tomography (SPECT) and CT fusion has become commercially available. The concept of combining SPECT studies with CT acquired during a single examination has stimulated a great deal of productive basic and clinical research [1]. Several companies are now offering these instruments, which include the GE Hawkeye system (GE Healthcare, Haifa, Israel), the Symbia system (Siemens Medical Solutions, Hoffman Estates, IL, USA), and the Precedence system (Philips Medical Systems, Milpitas, CA, USA). The development principle of various SPECT/CT devices and important considerations such as attenuation correction and co-registration are discussed in the first section of this article.

Although the system started later than PET/CT, SPECT/CT has many existing and potential areas of clinical application and has significantly added to the diagnostic power of nuclear medicine. The specific disease processes where SPECT/CT has had positive impact on diagnostic accuracy are illustrated in this article. Examples include infection studies with gallium-67 citrate (^{67}Ga), bone imaging with ^{99m}Tc-methylene diphosphonate (^{99m}Tc-MDP), ^{99m}Tc-sulfur-colloid (^{99m}Tc-S-colloid) sentinel lymph node mapping, thyroid cancer survey with ^{131}I-sodium iodide (^{131}I), and parathyroid scan with ^{99m}Tc-Sestamibi (^{99m}Tc-MIBI) (Table 1).

2. SPECT/CT principles and instrumentation

The advantages of combining SPECT with CT are numerous and are primarily due to the anatomic referencing and attenuation correction capabilities of CT. Technical developments over the past 20 years have led to the development of better software techniques for image fusion. While hardware image fusion techniques have been in clinical use for many years, the first commercial SPECT/CT system was the GE Hawkeye system (GE Healthcare), which was developed in 1999 [2].

There are varying technical issues surrounding the different SPECT/CT devices, ranging from cost, radiation dosages, treatment planning, and sitting requirements to system-specific issues such as table sag and CT artifacts due to patient motion. As this technology matures, we can expect to see a range of SPECT/CT devices available on the market that range from low-dose 1–4 slice inexpensive CT upgrades of conventional SPECT systems, to SPECT systems incorporating 64- or 128-slice CT scanners. The justification for such devices will be heavily dependent on clear demonstration of their value in clinical practice [3].

Much of the early work on the development of a combined SPECT/CT unit was performed at the University of California, San Francisco by Hasagawa et al [4] and Lang et al [5] in the early 1990s. Their initial work focused on the development of a system

Table 1 — Clinical applications and abbreviations of radiopharmaceuticals for SPECT images mentioned in this review

Radiopharmaceuticals	Abbreviation	Clinical applications
Gallium-67 citrate	^{67}Ga	Inflammation and tumor scan
Technetium-99m methylene diphosphonate	^{99m}Tc-MDP	Bone scan
Technetium-99m sulfur colloid	^{99m}Tc-S-colloid	Sentinel lymph node Liver-spleen scan
Technetium-99m sestamibi	^{99m}Tc-MIBI	Parathyroid scan Myocardial perfusion scan
Technetium-99m ethyl cysteinate dimer	^{99m}Tc-ECD	Cerebral perfusion scan
Technetium-99m TRODAT	^{99m}Tc-TRODAT	Brain dopamine transporter scan
Technetium-99m dimercaptosuccinic acid	^{99m}Tc-DMSA	Renal cortical scan
Technetium-99m labeled red blood cell	^{99m}Tc-RBC	Gastrointestinal bleeding scan
Technetium-99m fanolesomab	^{99m}Tc-fanolesomab	Infectious scan
Technetium-99m ciprofloxacin	^{99m}Tc-ciprofloxacin	Infectious scan
Iodine-131 sodium iodide	^{131}I	Thyroid scan Thyroid cancer work-up
Iodine-131 metaiodobenzylguanidine	^{131}I-MIBG	Adrenal medulla scan

that could perform simultaneous CT and SPECT studies. Their work highlighted, for the first time, the potential benefits of a single device capable of performing anatomic and functional imaging. They demonstrated that such a system was capable of performing attenuation correction and could permit accurate quantification of radiotracer activity in a porcine myocardium (6). This group was also the first to build a combined SPECT/CT system for clinical studies (7). This system used a single-slice CT scanner and a single-head large field of view gamma camera and was the forerunner of today's systems that combine a multidetector CT (MDCT) system and dual-detector SPECT system.

2.1. SPECT/CT devices in clinical service

2.1.1. Low current CT add-on conventional SPECT system

The first commercial SPECT/CT system was the GE Hawkeye system (GE Healthcare), which was developed in 1999 (2). This system took advantage of the unique slip-ring gantry of the system to mount an X-ray tube emitting a fan-beam of radiation on detectors at the opposite sides of the slip-ring gantry. The mechanical constraints placed by the heavy detectors limited the CT rotational speed. For a transaxial slice, each slice had an axial thickness of 10 mm. The X-ray system operated at 140 kVp with a tube current of 2.5 mA. Although this resulted in a significantly lower patient dose by a factor of 4 to 5, the quality of the CT images were inferior to that of state-of-the-art CT scanners (3).

The recently developed Hawkeye-4 (Fig. 1A) uses the same gantry as the original Hawkeye system and acquires four 5-mm thick slices with each rotation instead of one 10-mm slice. This design retains the very compact design of the Hawkeye system, delivers a low radiation dose to the patient and requires minimal room shielding (3). The primary purpose of the Hawkeye system was not image fusion but rather the production of a high-quality attenuation map for use with the emission data. In this respect, the slow scan speed was advantageous in that breath holding was not possible and the CT images were blurred by respiratory and cardiac motion in a comparable manner to the SPECT raw data. As of the end of March 2008, six Hawkeye-4 systems have been installed in hospitals in Taiwan.

2.1.2. Integrated SPECT/CT systems with high-quality CT

Two vendors have opted for the development of SPECT/CT systems that are more comparable to their PET/CT counterparts, with the goal of providing high-quality CT images fused to the SPECT image data. The Precedence system from Philips Medical Systems couples a conventional 6-slice or 16-slice CT scanner to their dual-detector Skylight system. So far, no Precedence system has been installed in Taiwan.

The Symbia system (Siemens Medical Solutions) incorporates 1-, 2- or 6-slice CT scanners with their dual-detector E-Cam system (Fig. 1B) (3). With both systems, CT slice thickness is variable and can be adjusted from 0.6 mm up to 10 mm. The scan speed

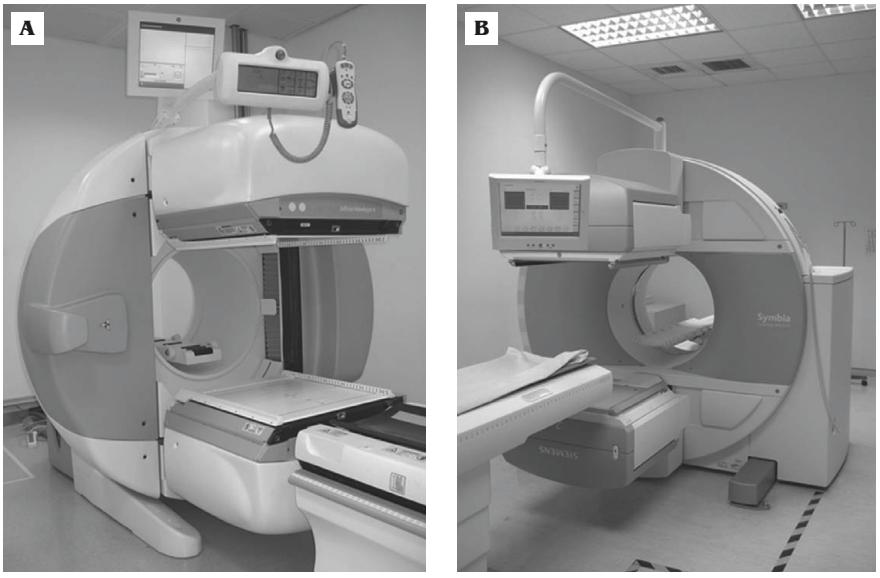

Fig. 1 — (A) The GE Hawkeye 4® system installed in Tzu Chi General Hospital. The X-ray tube housing is seen on the left side of the gantry with the array of detectors on the right side. (B) The Siemens Symbia® system installed in National Taiwan University Hospital. This is an integrated gantry that contains a multidetector row CT system and dual-detector E-Cam system (courtesy of Dr Kai-Yuan Tzen at the National Taiwan University Hospital, Taipei, Taiwan).

for a 40-cm axial field of view is less than 30 seconds. In comparison, the CT scan time on the GE Hawkeye-4 system is 5 minutes for a 40-cm field of view (3). However, because of the addition of a separate CT gantry, both the Symbia and Precedence systems are considerably larger than the conventional SPECT systems and have very different sitting and shielding requirements compared with the GE Hawkeye system. As of the end of March 2008, three Symbia systems have been installed in hospitals in Taiwan. Whether the CT component in the combined imaging approach should be a conventional MDCT scanner or the more compact, low current CT add-on used in the GE Hawkeye system is currently still a matter of debate.

3. Advantages of SPECT/CT: attenuation correction and anatomic referencing

The advantages of combining SPECT with CT are primarily due to the attenuation correction and anatomic referencing capabilities of CT (see below). Due to these two purposes, ensuring that the CT and SPECT images are correctly co-registered in three dimensions is important.

3.1. Attenuation correction

To correct SPECT images for attenuation, the spatial distribution of attenuation coefficients within the patient must be known. This attenuation map is then incorporated into a statistically based, iterative reconstruction algorithm such as ordered subset expectation maximization (OSEM) (8,9). In the current SPECT/CT system, the spatial distribution of attenuation coefficients is measured using a CT scanner. With any type of CT system, the image noise in attenuation maps is very low, and the in-plane resolution is high compared with maps generated from radionuclide-based transmission systems. Although CT systems generate a higher resolution map, improvement in the resolution is not necessarily a factor in the accuracy of the attenuation compensation because we are primarily concerned with obtaining an accurate estimation of the attenuation path length for each pixel in the SPECT transaxial data (3).

For the use of attenuation correction, the most frequent clinical studies include cerebral perfusion imaging with ^{99m}Tc-ethyl cysteinate dimer (^{99m}Tc-ECD) and brain dopamine transporter imaging with ^{99m}Tc-TRODAT. Special attention has to be paid with regard to the possible mis-registration between the CT and SPECT images causing errors on attenuation correction. However, we would like to focus this review on the clinical applications and usefulness of integrated SPECT/CT imaging. We leave the discussion of the physics and instrumental aspects of the SPECT/CT scan for attenuation correction and technical issues causing possible pitfalls to future papers from our group.

3.2. Anatomic referencing

For co-registration of anatomic and functional information, the accurate co-registration of the SPECT and CT data are just as important as with the attenuation correction. Many of the pitfalls such as patient motion as well as respiratory and cardiac motion all apply equally to image fusion. Usually, a calibration procedure is needed to ensure that both the CT and SPECT images are correctly co-registered in three dimensions. For the GE Hawkeye-4 system, a series of six syringes containing an appropriate radionuclide are inserted into a foam calibration phantom so that they are orientated in three orthogonal planes (Fig. 2). After SPECT/CT acquisition, the software is used to automatically determine the location of the syringes and either computes the necessary calibration factors to ensure precise alignment of the CT and SPECT images or, on a routine basis, confirms the validity of the existing calibration factors. This type of calibration procedure is essential if the clinician is to have confidence in the ability of the technology to permit accurate localization of radiotracer uptake in the body (3).

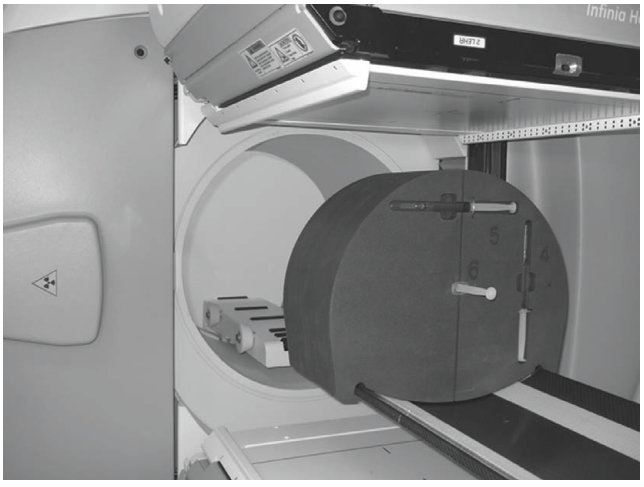

Fig. 2 — To ensure that the CT and SPECT images are correctly co-registered in three dimensions, a series of 6 syringes (3 of which can be seen in the photograph, the other 3 are on the reverse side of the phantom) containing an appropriate radionuclide are inserted into a foam calibration phantom so that they are orientated in three orthogonal planes. When imaged on both the SPECT and CT systems, they permit accurate alignment of the CT and SPECT data. The calibration system is used for the GE Hawkeye 4 system.

For the use of anatomic referencing, the most frequent clinical studies include infection studies with ^{67}Ga-citrate, thyroid cancer survey with ^{131}I, and parathyroid scan with ^{99m}Tc-MIBI, ^{99m}Tc-S-colloid sentinel lymph node mapping, and bone imaging with ^{99m}Tc-MDP. In the text, the authors give some examples of the routine clinical applications of SPECT/CT at the Tzu Chi General Hospital, Taipei Branch.

4. Clinical usefulness of SPECT/CT fusion imaging

4.1. Infection and inflammation

Two of the well-known radiopharmaceuticals used for the detection and localization of infection/inflammation are ^{67}Ga-citrate and radiolabeled white blood cells (WBCs). Newer agents such as radiolabeled monoclonal antibodies, most commonly ^{99m}Tc-fanolesomab [10] and ^{99m}Tc-ciprofloxacin [11,12], and ^{18}F-fluorodeoxyglucose (FDG) [13,14] have the potential for faster and more specific diagnoses. These radiopharmaceuticals reflect physiologic and pathologic functions rather than anatomic abnormalities. In the clinical setting, it is often necessary to correlate these functional studies with anatomic imaging. ^{67}Ga-citrate is a readily available radiopharmaceutical. It is easy to handle, unlike radiolabeled WBCs, requiring no blood sampling, labeling, and re-injection of blood products. ^{67}Ga is an iron analog [15]; it binds to iron-binding proteins of inflammatory cells, bacterial siderophores, or other mucopolysaccharide proteins [16].

For disseminated infectious lesions, the planar whole body ^{67}Ga scan is useful for detecting multiple lesions in a single examination [17]. For some specific anatomic structures, ^{67}Ga activity can be used to identify the specific pattern of uptake such as psoas abscess (Fig. 3) [18] or aortic arch septic aneurysm (Fig. 4) [19]. However, most of the ^{67}Ga uptake lesions need further co-registration to bone or other imaging modalities [20–22].

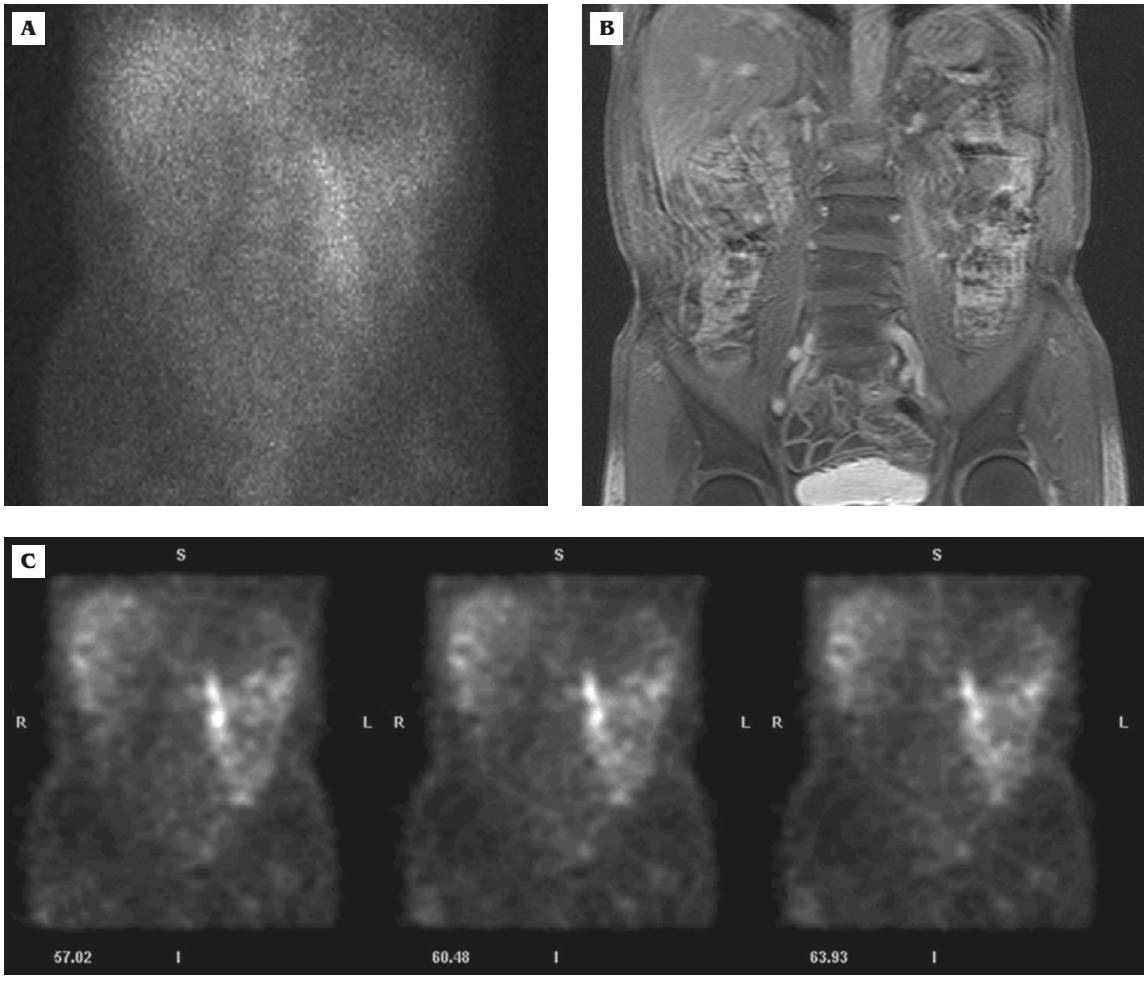

Fig. 3 — (A) Planar ^{67}Ga scan revealed a band-shaped focal uptake in the paraspinal region, the direction of the lesion corresponding to the psoas muscle. (B) Magnetic resonance imaging revealed left psoas muscle abscess. (C) Serial coronal sections of ^{67}Ga SPECT over the abdominal region confirmed the diagnosis of left psoas muscle abscess.

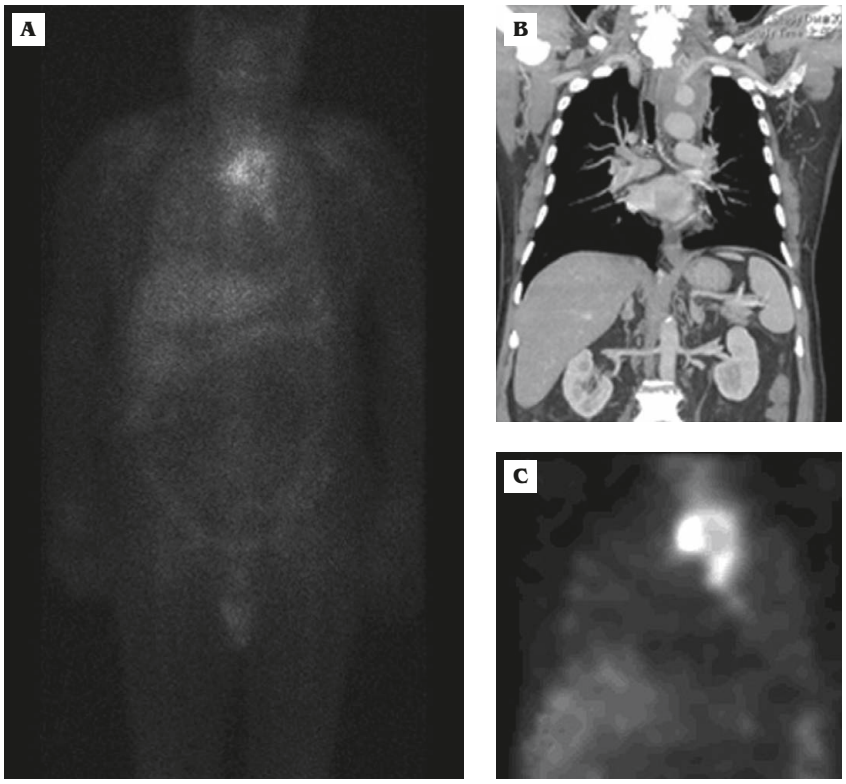

Fig. 4 — (A) Planar ^{67}Ga scan revealed an arch-like focal uptake in the upper mediastinal region, the shape of the lesion corresponding to the aortic arch in the upper chest region. (B) Chest CT showed mediastinal abscess with mycotic aneurysm of the aortic arch and subclavian artery. (C) Serial coronal sections of chest ^{67}Ga SPECT revealed that the arch-like ^{67}Ga-avid lesion corresponded to the aortic arch.

The advent of SPECT provides tomographic images for direct correlation to CT and magnetic resonance imaging (MRI) anatomic modalities. Integrated SPECT and CT increase the specificity of the physiologic modality and increase the sensitivity of the anatomic modality. In one of the earlier studies, Swayne performed a prospective evaluation of software SPECT and CT fusion in 10 patients with suggested inflammatory disease (23). Correct localization was found in all 10 patients, suggesting that the method is an accurate one of functional and anatomic correlation. Several subsequent investigations have shown that SPECT/CT fusion is beneficial to the interpretation in a majority of cases and increases sensitivity and specificity (24). With integrated SPECT/CT images, ^{67}Ga uptake lesion involved in the tissues and organs can be clearly identified using CT images (Figs. 5 and 6).

4.2. Endocrine tumors

The introduction of SPECT/CT into the field of endocrinology led to a major breakthrough in the diagnosis and management of patients with endocrine tumors. The scintigraphic functional techniques for the diagnosis of endocrine tumors are mainly associated with the unique uptake and transport mechanisms and with the presence of high densities of membrane receptors on some of these tumors, which reflect the pathophysiologic status of the disease process. However, lack of structural delineation and relatively low contrast may mix up the localization of the abnormal functional findings with the physiologic biodistribution of the radiotracers. In the past, simultaneous dual-tracer image such as combined ^{131}I-metaiodobenzylguanidine (^{131}I-MIBG) and ^{99m}Tc-MDP bone scan or ^{99m}Tc-dimercaptosuccinic acid (^{99m}Tc-DMSA) renal cortical scan for localization of pheochromocytoma or neuroblastoma (25,26), failed to provide accurate anatomic localization of neuroendocrine tumors.

Anatomic high-resolution and functional imaging data acting as complementary methods led to various combination techniques of these modalities. SPECT/CT enables the sequential acquisition of the two modalities, with subsequent merging of data into a composite image display. We present two examples of the contribution of integrated SPECT/CT technology for image analysis and management of patients with well differentiated thyroid cancer (WDTC) and parathyroid adenoma.

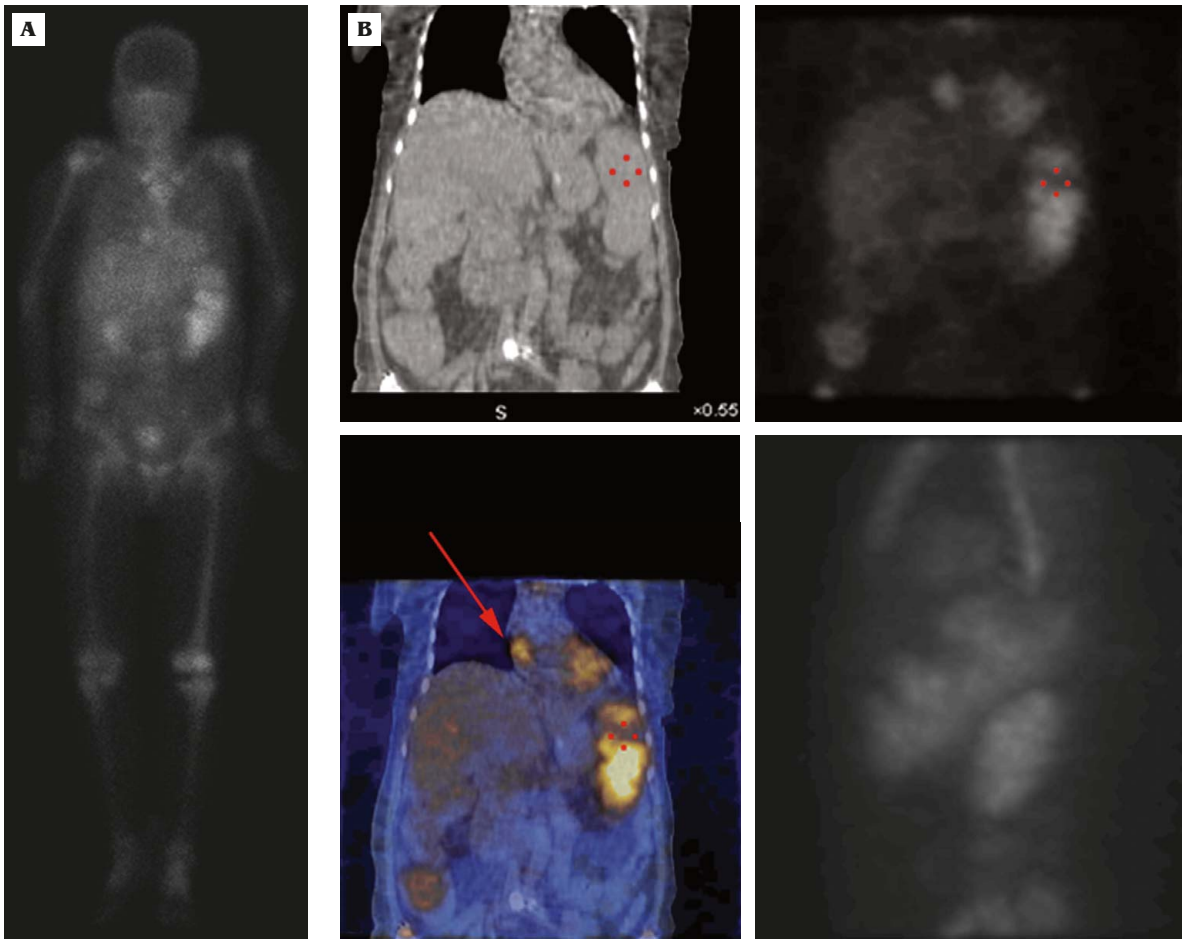

Fig. 5 — A 76-year-old female with urinary tract infection and persistent fever after treatment was referred for ^{67}Ga whole body survey. Abdominal CT showed splenomegaly with multifocal hypodense areas in the splenic parenchyma and prominent of uterus cavity, splenic infarction was suspected. (A) Whole body ^{67}Ga scan revealed multiple areas of increased ^{67}Ga accumulation involving the right cardiac region, spleen, bilateral kidneys, and lower pelvis around the uterus region. Disseminated infectious foci were diagnosed. (B) ^{67}Ga SPECT/CT over the lower chest to upper abdominal region demonstrated abnormal splenic ^{67}Ga accumulation with segmental cold defects (asterisk) suggestive of diffuse splenic infection with focal infarctions. The right cardiac lesion also became more prominent in the SPECT/CT images (red arrow).

4.2.1. ^{131}I SPECT/CT for WDTC

Whole body ^{131}I scanning can be used to detect residual or recurrent WDTC and metastatic tumor before visualization on anatomic imaging modalities. ^{131}I-avid malignant foci can then be removed surgically or be treated with high doses of ^{131}I. Because of a lack of anatomic landmarks, abnormalities detected on ^{131}I planar whole body scan and SPECT are difficult to interpret. Normal active radioiodine transport in the salivary glands, nasopharynx, gastric mucosa, and breast tissue may cause missed diagnosis of WDTC lesions. Diagnostic pitfalls leading to the need for additional images or diagnostic procedures were found in 59% of a total of 500 whole-body ^{131}I scans from 300 consecutive patients, mainly as the result of contamination, intestinal retention, hot nose, unexpected breast activity (27), as well as kidney and isolated peripheral metastasis (28).

The incremental value of SPECT/CT was documented in a preliminary report of 54 patients who underwent 67 SPECT/CT studies along with 565 ^{131}I whole body scans of 298 patients with WDTC during a 40-month period (29). SPECT/CT was performed in these patients when an extrathyroidal ^{131}I-avid site could not be attributed to physiologic uptake or to a well-defined metastasis (Fig. 7). SPECT/CT contributed to image interpretation of 54 among the 80 ill-defined ^{131}I-avid foci (68%) in 38 patients (70%), mainly in cervical nodes, pelvic soft tissue and bone. SPECT/CT affected the management of 22 patients (41%). These management changes included: (1) diagnosis of bone metastasis led to radiation therapy in three patients; (2) identification of resectable tumor mass for surgery in three patients; (3) and avoidance of unnecessary ^{131}I treatment after the recognition of physiologic ^{131}I activity in 16 patients (29).

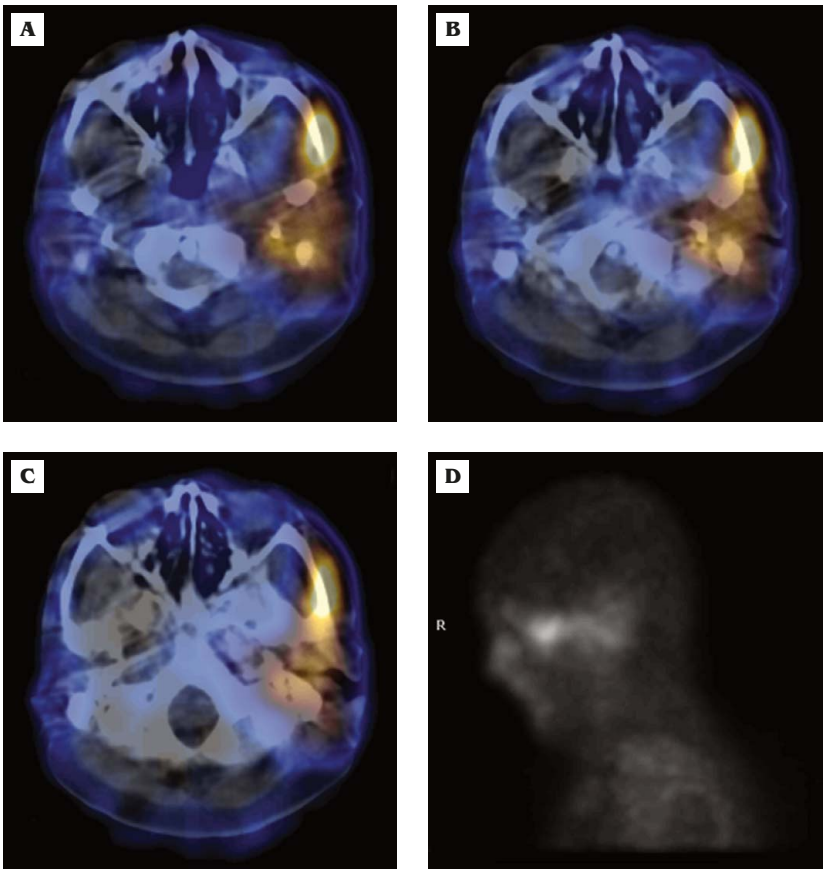

Fig. 6 — A 73-year-old diabetic man with left facial palsy was diagnosed with necrotizing otitis media which suggested skull base and temporal bone involvement. Whole body ^{67}Ga scan was performed to determine the territory of infection involvement. (A, B, C) Serial transaxial sections of ^{67}Ga SPECT/CT fusion images and (D) left lateral projection image over the skull revealed that the ^{67}Ga-avid lesion involved the arch of the left zygomatic bone to the left external and middle ear, left masticator space, and mastoid region, compatible with otitis media with adjacent skull base bone and soft tissue involvement.

In another study of 25 patients with inconclusive whole body findings after ablative radioiodine therapy, SPECT/CT improved the anatomic assignment in 17 of 39 sites (44%) with changes in management in six of 24 (25%) patients (30). When we compared ^{131}I SPECT/CT to planar imaging in 71 patients, incremental value of SPECT/CT was documented in 41 of the 71 patients (57%). Major changes in management were observed when SPECT/CT provided better localization of ^{131}I uptake to lymph node metastases versus remnant thyroid tissue, to the lung versus mediastinal metastases, and to the skeleton (31).

With an anterior upper mediastinal mass, the differential diagnoses included thymoma, teratoma, thyroid tumor or goiter, and lymphoma. The authors used low-dose ^{131}I SPECT/CT to define a huge upper mediastinal tumor as an intrathoracic goiter. The ^{131}I SPECT/CT images correlated well with diagnostic CT and confirmed the diagnosis of intrathoracic goiter (Fig. 8).

4.2.2. ^{99m}Tc-MIBI SPECT/CT for localizing parathyroid adenoma

^{99m}Tc-MIBI is a lipophilic cationic complex used primarily for the detection of myocardial perfusion abnormalities. ^{99m}Tc-MIBI also accumulates nonspecifically in various tumors, such as breast tumors and parathyroid adenomas. Although the exact mechanism is not fully understood, mitochondria have been implicated in its uptake by parathyroid cells (32). Also, the sizes and cellularity of the abnormal glands correlated with the uptake of ^{99m}Tc-MIBI (33).

Parathyroid adenomas account for 85% of hyperparathyroidism cases. Preoperative localization of parathyroid adenomas has gradually become important since the widespread use of minimally invasive surgical procedures in patients with primary hyperparathyroidism. Minimally invasive procedures have been associated with decreased risk of hypoparathyroidism and of recurrent laryngeal nerve injury, as well as shortening of surgery time and hospitalization.

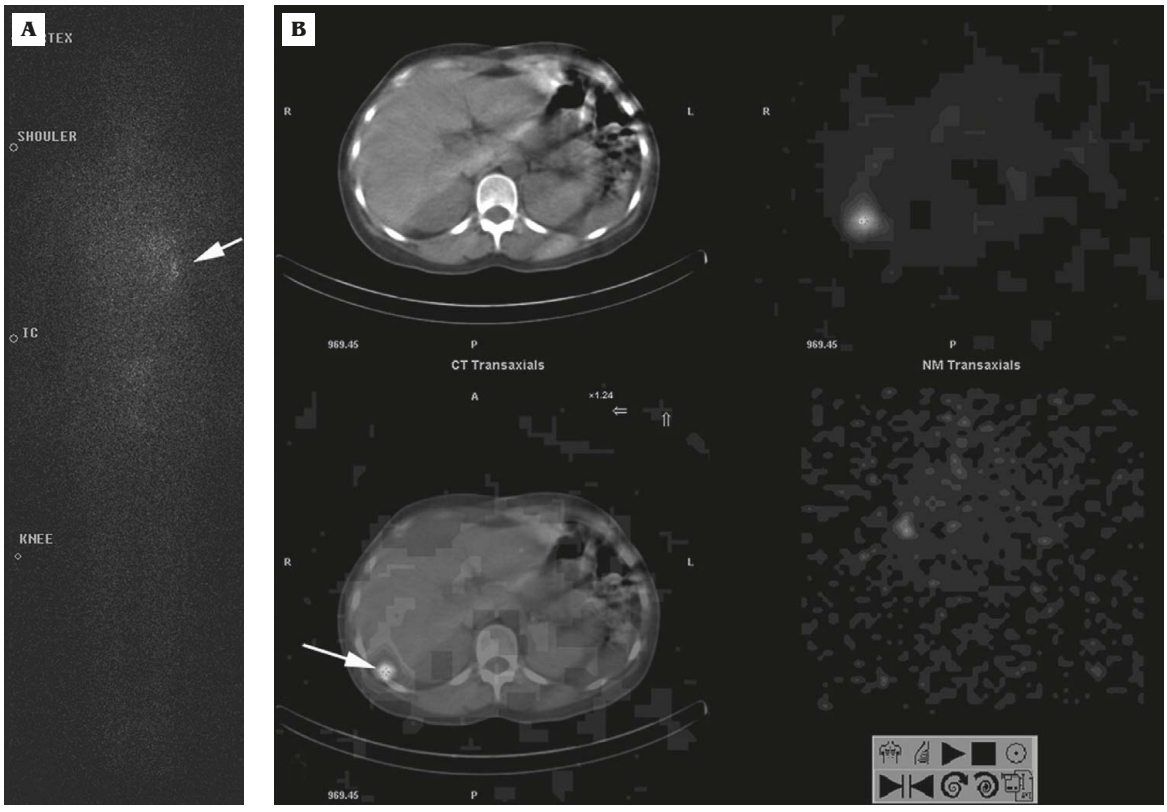

Fig. 7 — (A) Posterior view of a low-dose ^{131}I whole-body scan of a 35-year-old female WDTC patient shows a focal area of abnormal ^{131}I accumulation in the right mid portion of the body (arrow). (B) Transaxial SPECT/CT imaging over the lower chest to upper abdominal region revealed that the ^{131}I-avid lesion was localized in the right lobe of the liver on the fusion image (arrow). The results of SPECT/CT indicated the need for large-dose ^{131}I therapy.

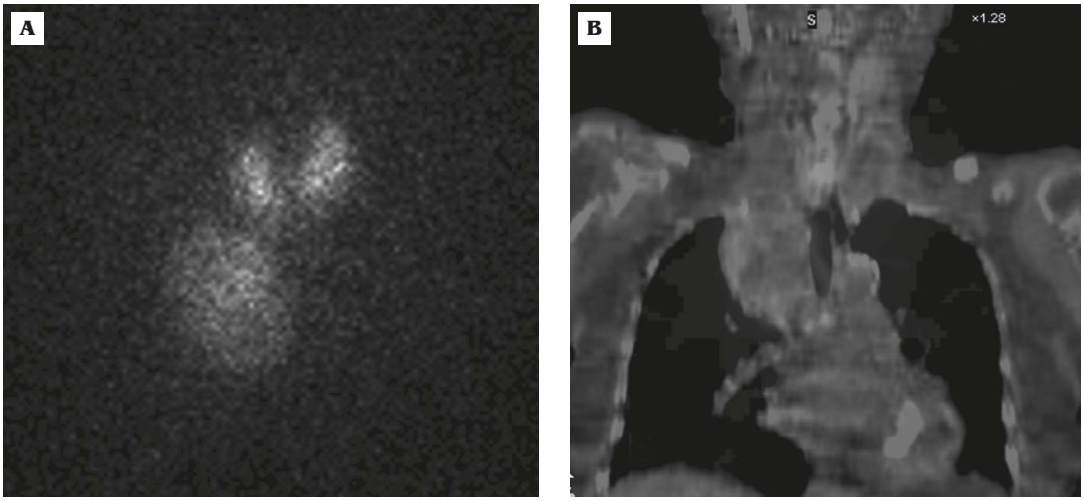

Fig. 8 — A 75-year-old female was diagnosed to have a large upper mediastinal mass on chest CT. ^{131}I thyroid scan was performed to rule out intrathoracic goiter. (A) Low-dose ^{131}I revealed normal thyroid glands with a huge heterogeneous ^{131}I accumulation lesion in the right upper chest region. (B) Coronal view of the ^{131}I SPECT/CT fusion image revealed that the upper chest ^{131}I accumulation corresponded to the upper mediastinal mass found on diagnostic chest CT.

The limited surgical procedures include minimally invasive parathyroidectomy, endoscopic surgery [34], and video-assisted thoracic surgery for resection of ectopic mediastinal parathyroid glands [35].

In the late 1990s, planar ^{99m}Tc-MIBI scintigraphy was confirmed to play a major role in the preoperative localization of parathyroid adenomas [36,37]. It is believed that the combined approach of planar

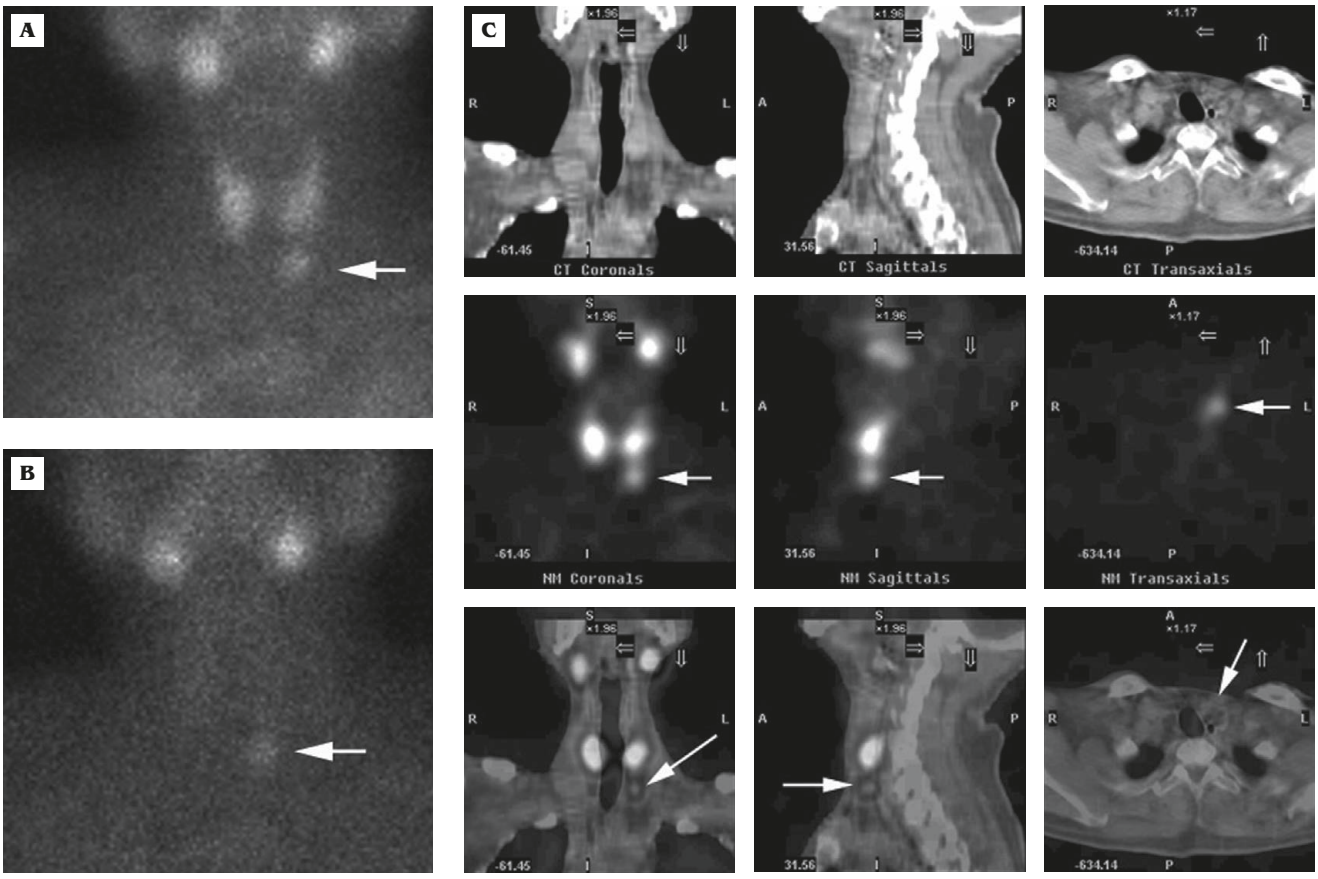

Fig. 9 — ^{99m}Tc-MIBI dual-phase parathyroid scan (A) at 10 minutes and (B) 2 hours after injection of the radioagent revealed a focal area of abnormal radioactivity uptake and retention inferior to the left lobe of the thyroid. (C) ^{99m}Tc-MIBI SPECT/CT images (displayed from left to right in coronal, sagittal, and transaxial sections, respectively) clearly demonstrated the anatomic location of the parathyroid adenoma. The multipanel display format provides surgeons with more informative ectopic parathyroid adenoma location for better preoperative planning.

^{99m}Tc-MIBI and ultrasonography (US) is considered the diagnostic strategy of choice for noninvasive detection of parathyroid adenomas located in the neck, with a sensitivity of 83% for US and 85% for subtraction MIBI, and increasing to 94% when using the combined imaging approach [38].

In addition to planar ^{99m}Tc-MIBI scintigraphy, ^{99m}Tc-MIBI-SPECT reached 96% sensitivity, superior to that of planar imaging (79%) [39]. However, even ^{99m}Tc-MIBI SPECT may not provide detailed anatomic information; therefore, co-registration of ^{99m}Tc-MIBI and CT has been suggested. In a study of 48 patients with primary hyperparathyroidism, SPECT/CT data were compared with those of SPECT only. SPECT-only imaging identified 89% of the surgically confirmed diseased parathyroid glands, and SPECT/CT improved localization of parathyroid adenomas in four patients (8%). SPECT/CT was particularly helpful in locating two ectopic parathyroid adenomas (Fig. 9) [40]. The usefulness of SPECT/CT in ectopic parathyroid adenomas was reported in a study of 36 patients with primary hyperparathyroidism [41]. ^{99m}Tc-MIBI SPECT/CT facilitated surgical exploration in all 10 ectopic parathyroid adenomas, but only in four of 23 cervical adenomas. In these 10 patients with lower neck/mediastinal parathyroid adenomas, SPECT/CT identified their proximities to the trachea, esophagus, thymus, spine, or sternum and optimized the surgical procedure in these patients. In addition, SPECT/CT facilitated the surgical resection of four adenomas in a subgroup of six patients scheduled for re-exploration after failed initial surgery. SPECT/CT provides better definition of organs and tumors that take up the radiotracers and of their precise relationship with adjacent structures, defines the functional significance of CT lesions and improves the specificity of SPECT by excluding diseases at sites of physiologic uptake or excretion.

4.3. Abdominal disease

In SPECT studies of abdominal diseases, SPECT/CT can play a role in the differential diagnosis of hepatic

hemangiomas located near vascular structures, in precisely detecting and locating active splenic tissue caused by splenosis in splenectomy patients, in providing important information for therapy optimization in patients undergoing hepatic arterial perfusion scintigraphy, in accurately identifying the involved bowel segments in patients with inflammatory bowel diseases, and in correctly locating the bleeding sites in patients with gastrointestinal bleeding (42).

4.3.1. Hepatic hemangioma

Hemangioma is the most common benign tumor of the liver. According to an autopsy series, its prevalence ranges from 3% to 20% (43). ^{99m}Tc-labeled red blood cell (^{99m}Tc-RBC) scintigraphy has proven to be an accurate and cost-effective noninvasive method to detect hepatic hemangiomas. It is able to improve the specificity of other imaging studies with a positive predictive value approaching 100% (44). Because of its high specificity for the noninvasive diagnosis of hepatic hemangiomas, ^{99m}Tc-RBC scintigraphy can spare the patient an invasive angiogram or biopsy of a vascular mass. However, even on SPECT imaging, the sensitivity of this technique is limited to lesions smaller than 1 cm and those located in unfavorable topographic sites (45).

With software SPECT and CT/MRI fusion images of 20 patients with 35 known hemangiomas, Birnbaum et al demonstrated the ease of identification of five of seven hemangiomas close to major intrahepatic blood vessels (46). The major clinical advantages of image fusion were the diagnostic confirmation of small hemangiomas and the correct characterization of hot-spots detected on SPECT studies adjacent to regions of vascular activity. However, the software fusion image process is time-consuming for the processing of accurate landmark positioning.

In 2004, Schillaci et al performed a study to verify whether new SPECT/CT hardware fusion images were able to improve ^{99m}Tc-RBC in patients suspected to have liver hemangioma (47). Twelve patients with suspected hepatic hemangiomas were studied. A total of 24 lesions were identified on SPECT, including 21 hemangiomas ranging from 0.6 cm to 4.2 cm in size; three hemangiomas (0.6 cm, 0.9 cm and 1 cm in size) were not identified on SPECT. In four (33.3%) of the 12 patients, the combination of using SPECT/CT added significant information compared with using SPECT alone. Moreover, SPECT/CT improved the accuracy of ^{99m}Tc-RBC scintigraphy in correctly classifying the hepatic lesions evaluated as hemangiomas or nonhemangiomas from 70.8% (17/24) to 87.5% (21/24).

In another study, Zheng et al demonstrated that SPECT/CT was used to correctly diagnose eight hemangiomas in less than ideal anatomic locations, including four close to the inferior cava, three close to the abdominal aorta, and one close to the heart. These lesions were clearly difficult to be correctly characterized using only SPECT (48).

4.3.2. Splenosis or accessory spleen

Splenosis is the autotransplantation of individual fragments of splenic tissue left behind after either operative or traumatic removal of the spleen (42). Experimental evidence has suggested that the presence of an intact spleen suppresses the growth and development of splenic implants. However, the existence of splenosis or accessory spleens may cause recurrence in patients who undergo splenectomy for hematologic diseases, i.e., idiopathic thrombocytopenic purpura or hemolytic anemia; thus, finding the correct location of active splenic tissue is important for subsequent surgical treatment (49).

Splenic scintigraphy with ^{99m}Tc-labeled radiocolloids or heat-damaged RBC is the most sensitive method for detecting active splenic tissue (50). Nevertheless, the precise locations of the sites of splenosis or accessory spleen may be very difficult to determine because of the lack of anatomic landmarks. This drawback may be overcome by integrated SPECT/CT imaging acquisition. Horger et al studied seven patients with history of either splenic trauma or splenectomy and hematologic disorders (51). They demonstrated that SPECT/CT improved diagnostic accuracy when it allowed for correct classification of indeterminate masses, or when previously unknown splenic implants were detected. SPECT/CT image fusion is important to establish the correct diagnosis, to increase observer confidence, and to plan surgical treatment.

In another study conducted by Valdes Olmos et al, they demonstrated that SPECT/CT was very useful for the diagnosis of ectopic splenic tissue simulating abdominal tumors in cancer patients (52).

4.3.3. Gastrointestinal bleeding

^{99m}Tc-RBC has been demonstrated to be clinically useful in the evaluation of patients with acute gastrointestinal (GI) bleeding (53). With regard to the usefulness of SPECT/CT in the detection of GI bleeding, Yama et al reported a case of intestinal bleeding in which fused images from ^{99m}Tc-RBC SPECT and from CT revealed small intestinal bleeding with specific anatomic features for a more precise definition of the location of the GI bleeding source (54). Integrated SPECT/CT imaging was able to furnish a high degree of specific anatomic information to scintigraphic data when conventional scans are positive for bleeding (Fig. 10). CT imaging identified structures and increased the specificity of ^{99m}Tc-RBC in the diagnosis of acute GI bleeding. Moreover, integrated SPECT/CT was useful for allowing better localization of Meckel's diverticulum using ^{99m}Tc-pertechnetate imaging to detect ectopic gastric mucosa as a source of lower GI bleeding (42).

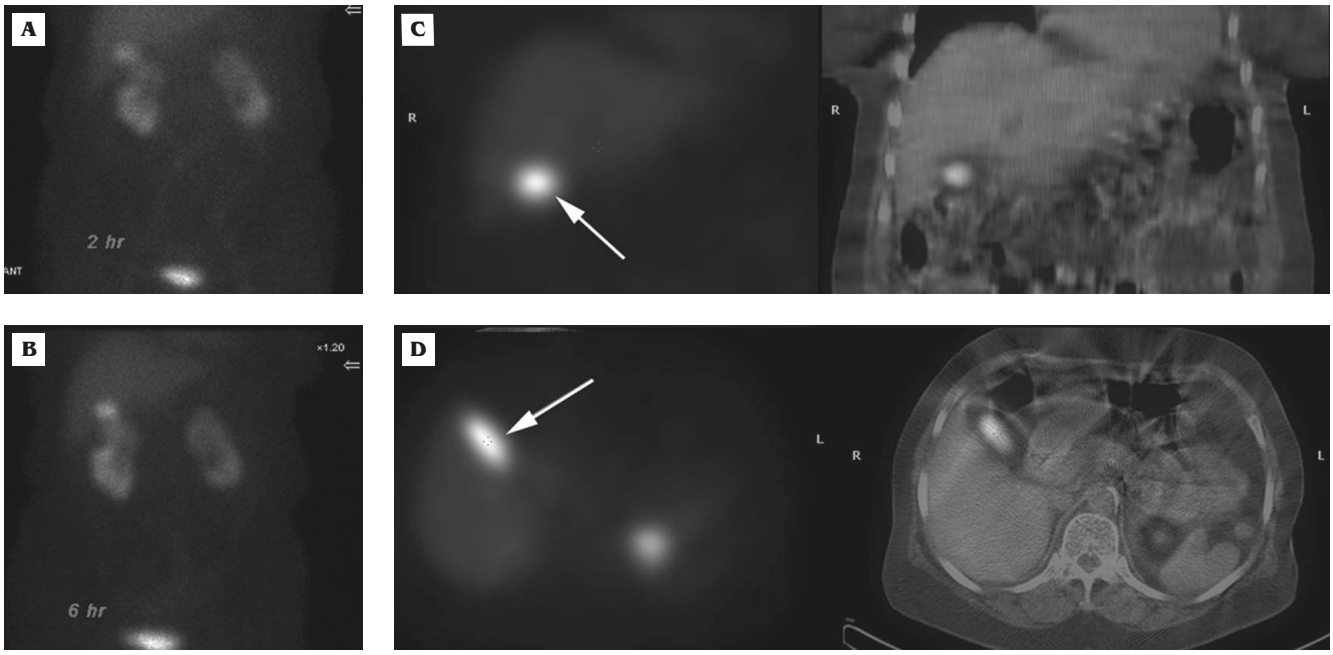

Fig. 10 — ^{99m}Tc-RBC abdominal scan at (A) 2 hours and (B) 6 hours after the injection of a radioagent revealed progressive accumulation of radiotracer in the upper right quadrant of the abdomen, in the lower margin of the right lobe of the liver. (C) Coronal and (D) transaxial ^{99m}Tc-RBC SPECT/CT fusion images 6 hours after injection of a radioagent revealed abnormal radioactivity accumulation in the gallbladder (arrows).

4.4. Sentinel lymph node mapping in breast cancer

The sentinel lymph node (SLN) is defined as the first node in the lymphatic drainage of the primary tumor. Tumor cells initially spread through the lymphatic pathway to one or more SLNs. Currently, in patients with breast cancer and malignant melanomas, SLN detection and biopsy have already been implemented into clinical practice (55,56). The precise anatomic location of SLNs is important for minimally invasive surgery and to avoid incomplete removal of the SLNs. All SLNs should be resected to achieve complete nodal staging. Minimally invasive SLN biopsies have successfully replaced lymphadenectomy for nodal staging (57,58). Therefore, precise anatomic localization of SLNs preoperatively is very important for successful surgical outcomes.

Conventional planar imaging using dynamic data acquisition (Fig. 11) is initially used to preoperatively identify the anatomic localization of the detected nodes. With the lack of anatomic outlines and body backgrounds, the certainty of the location of the nodes is still unsatisfactory. Even with the use of an intraoperative handheld gamma probe detector, a noninvasive technique that allows for better preoperative localization of SLNs and improvement in the detection rate is still needed.

With the use of SPECT/CT, combined metabolic and anatomic imaging in one single examination has been successfully used in SLN mapping (59,60). The results of SPECT/CT imaging can categorize the SLNs according to the American Joint Committee on Cancer by using the pectoralis minor muscle border between Level I/II and Level II/III. Therefore, even small hot spots with no body background can be precisely located. Husarik et al compared planar images, SPECT alone, and integrated SPECT/CT in SLN mapping in patients with breast cancer (59,60). As compared with planar images, SPECT/CT showed more accurate information in 34 patients (82%). In 29 patients (70%), the exact anatomic location was equivocal on planar images, whereas SPECT/CT showed the exact anatomic information needed to assign SLN levels. In six patients (14%), SLNs close to the injection site were detected with SPECT/CT; however, those were not visible on planar images due to scatter radiation. As compared with SPECT alone, SPECT/CT showed more accurate information in 26 patients (63%). In these 26 patients (63%), the exact anatomic locations were impossible to visualize on SPECT images alone. SLNs close to injection sites were not detected using SPECT alone in three patients (17%) but could be clearly delineated on SPECT/CT due to the anatomic correlation in the form of lymph nodes. Husarik et al concluded that localization and identification of SLNs was more accurate using integrated SPECT/CT imaging in comparison with planar images and SPECT images alone, respectively.

Lerman and coworkers compared planar images to SPECT/CT in SLN mapping of breast cancer in 157 patients (61). They found that 13% of SLNs were only

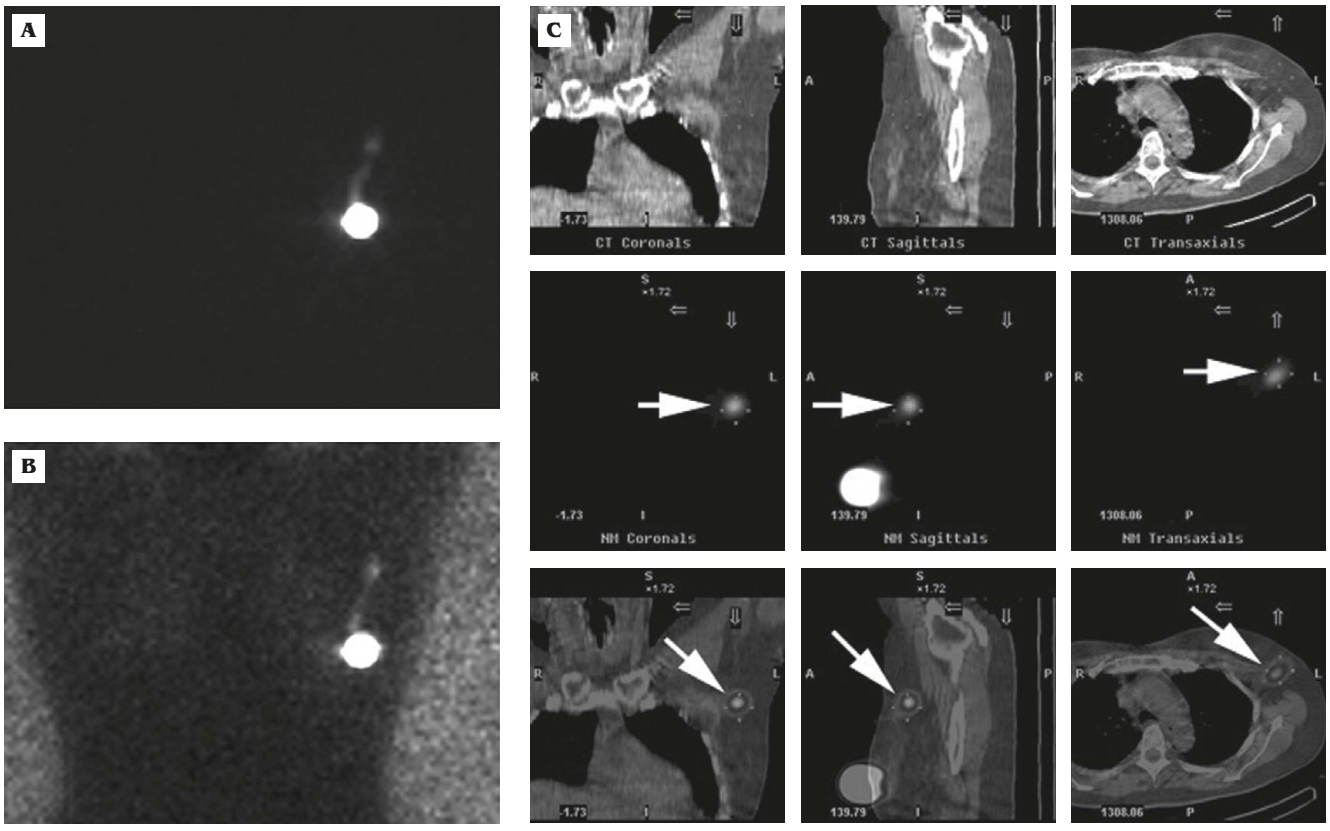

Fig. 11 — A 50-year-old woman with left breast cancer was scheduled to undergo SLN mapping before her surgery. (A) Summation of dynamic lymphoscintigraphy after injection of ^{99m}Tc-S-colloid subdermally above the breast tumor clearly shows SLN in the left axillary region. (B) Summation of dynamic lymphoscintigraphy with cobalt-57 (^{57}Co) radioactive flood source was used to outline the body shape for better localization of the SLN. (C) Three different section displays of SPECT/CT images through the SLN revealed better relative anatomic localization of the SLN (asterisk) to the pectoralis muscle on the CT images.

identified using lymphoscintigraphy on SPECT/CT due to the obscuring by scattered radiation from the injection site, and two SLNs were misinterpreted as one on planar images. In addition, unexpected sites of drainage were found in 33 patients.

From the literature review above, integrated SPECT/CT was clearly superior to SPECT alone or planar images, especially with regard to exact anatomic localization of SLNs. The high anatomic accuracy of integrated SPECT/CT facilitates the detection of SLN during minimally invasive surgery. SPECT/CT images might replace external marking of the SLN before surgery because of the high content of information of SPECT/CT images. With the newly developed imaging segmentation programs, SPECT/CT images can even co-register the SLN with the bone frame extracted from the CT images of SPECT/CT (Fig. 11) [62–64].

4.5. Bone tumor and malignant metastases survey

Whole body bone scans have been used clinically for more than 30 years and they are known as one of the most sensitive noninvasive methods for detecting focal bone pathology. In general, whole-body scans are used for bone scintigraphy, which permit the assessment of the overall distribution of the radiopharmaceutical. Both anterior and posterior studies are reviewed in parallel, thus, comparing any alterations, and noting eventual asymmetries on both sides of the midline. Additional spot views are obtained when specific clinical problems that need to be further clarified are detected on whole-body imaging. Under certain conditions, such as local symptoms suggestive of metastases, additional SPECT scans of the body area in question should be considered to increase diagnostic sensitivity. Accurate differentiation between benign and malignant lesions is of paramount importance, which indicates short or limited survival and the need for intensified treatment of malignant lesions (Fig. 12) [65].

In patients with high risk of bone metastases, additional anatomic information is often necessary. Particularly, bone lesions located in the spine and thoracic cage cannot be sufficiently assessed using conventional radiographic examinations and instead require the additional use of CT or MRI. SPECT/CT

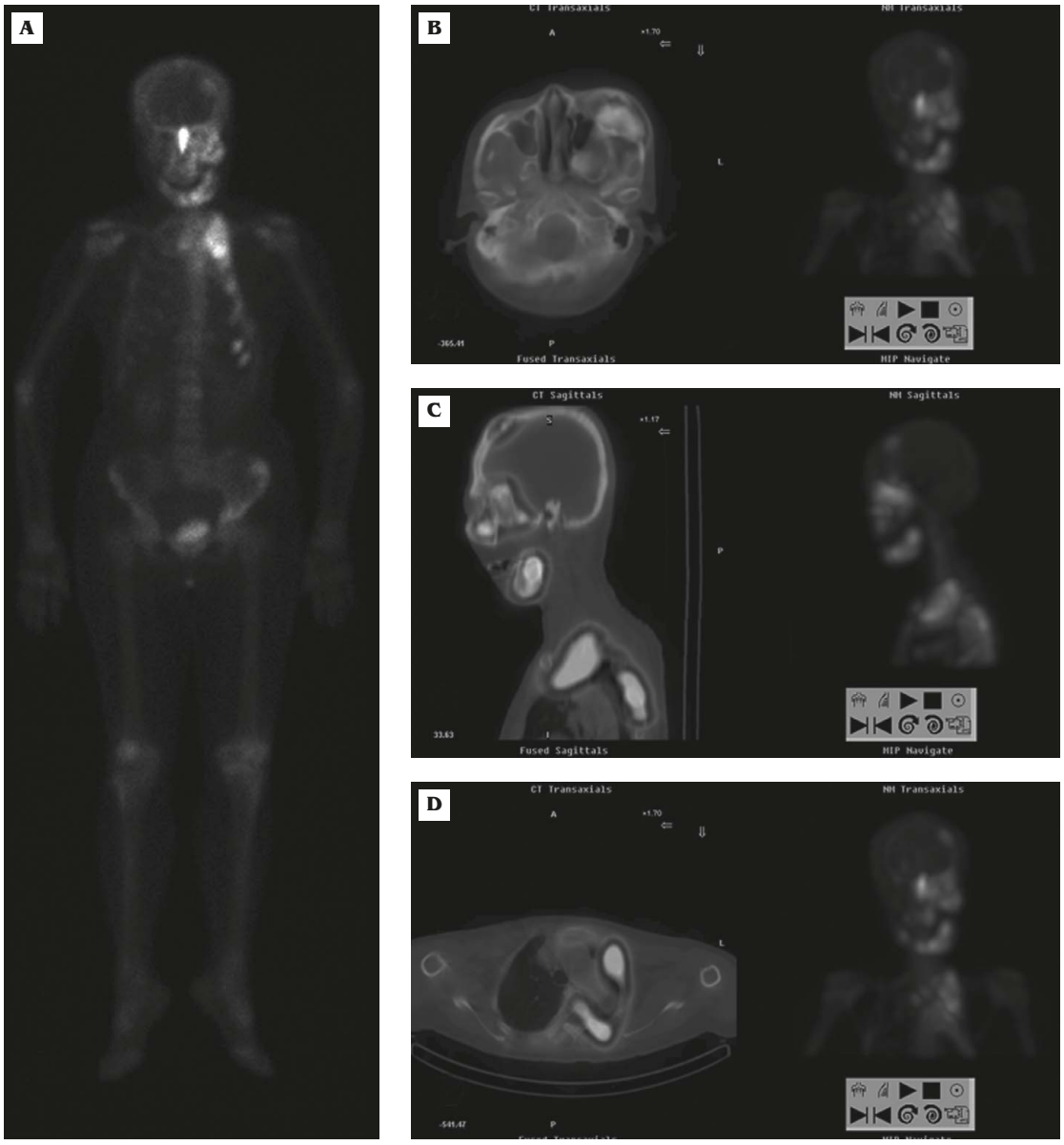

Fig. 12 — A 54-year-old woman with facial bone and chest wall deformities was referred for ^{99m}Tc-MDP bone scan. (A) Anterior view of the whole-body bone scan revealed multiple bone lesions involving the nasal bone of the skull, left hemifacial bones, left rib cage, and left hemipelvic bones. The bone scan findings were suggestive of polyostotic fibrous dysplasia. (B, C, D) ^{99m}Tc-MDP bone SPECT/CT fusion images clearly demonstrated the territory of these bone lesions which still underwent active remodeling. SPECT/CT is especially useful in the three-dimensional display of bone involvement in craniofacial bones. Bone biopsy over the facial bone confirmed the diagnosis of fibrous dysplasia.

imaging has proven to be extremely useful in identifying benign skeletal abnormalities, such as osteochondrosis, spondylopathy, or degenerative spondyl arthrosis, as the reason for abnormal tracer uptake. A benefit of SPECT/CT is to help define bone lesions to guide subsequent biopsy (65,66).

There have many unexpected findings in patients with cancer who are undergoing bone scintigraphy for staging. Extraosseous uptake associated with calcification might be found in some instances that cannot be correctly diagnosed without corresponding anatomic images. Extraosseous uptake has been described in amyloidosis, rhabdomyolysis (67), high voltage electrical burn (68), infarction of heart, spleen (Fig. 13), intestine (69), and soft tissue tumor (70,71). To differentiate this great variety of possible causes, morphologic information obtained by SPECT/CT is needed (65).

5. Conclusions

The concept of combining SPECT studies with CT acquired during a single examination has stimulated

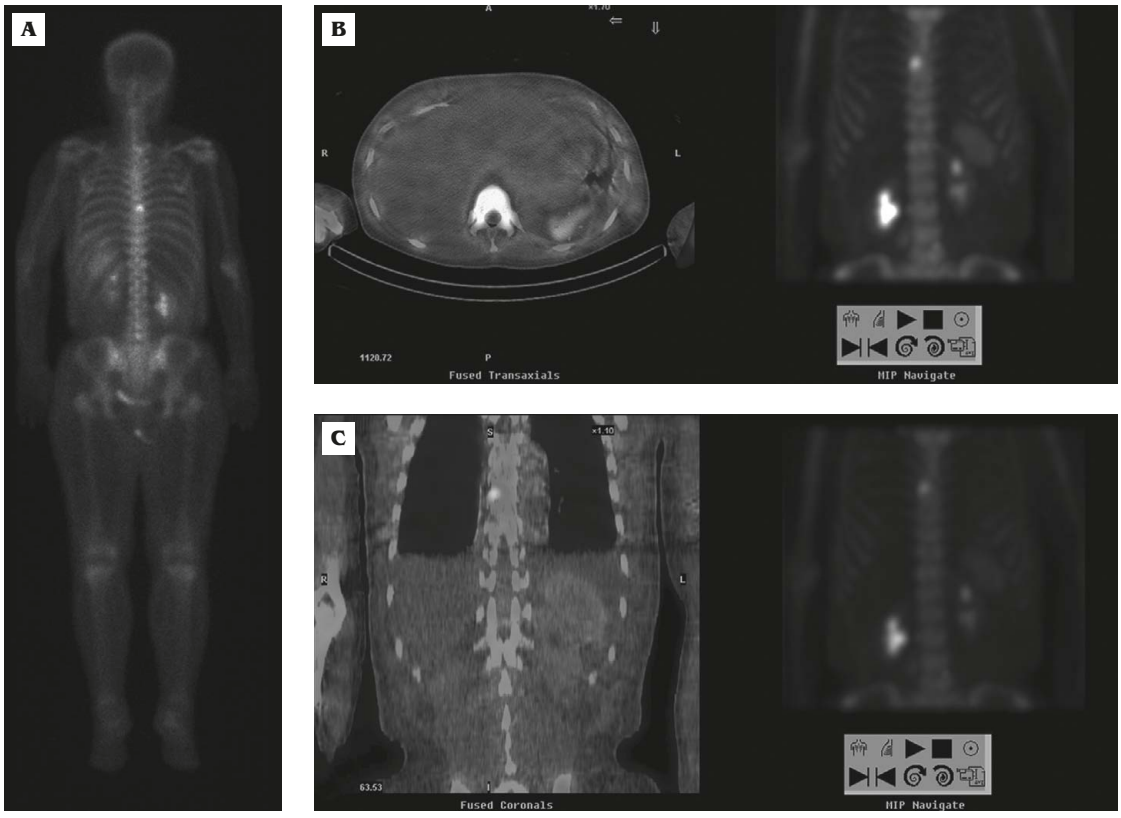

Fig. 13 — A 55-year-old woman with bilateral breast cancer after surgery and chemoradiotherapy was referred for ^{99m}Tc-MDP whole-body bone metastases survey. (A) Posterior view of whole-body bone scan revealed a T7 spine lesion with focal soft tissue uptake bone seeking agent in the upper left quadrant of the abdomen. (B) Transaxial and (C) coronal views of ^{99m}Tc-MDP SPECT/CT fusion images over the lower chest and upper abdominal region revealed a soft tissue mass in the upper left quadrant of the abdomen corresponding to the spleen metastasis (asterisk in B).

a great deal of productive basic and clinical research which has resulted in successful clinical applications in a variety of diseases. In this review article, the authors focused on specific disease processes where SPECT/CT has had a positive impact on diagnostic accuracy and is currently being used in Tzu Chi General Hospital, Taipei Branch.

Hopefully, the specific role of SPECT/CT will continue to emerge as utilization of this approach increases. Close and cooperative relationships between clinical physician and nuclear medicine physician are essential to the growth of SPECT/CT use in the coming decade.

Acknowledgments

The authors would like to thank Mr Chih-Yi Wu, Mr Wen-Hsiang Chou, Mr Jia-Hung Li, and Miss May-Yin Wong for their excellent technical support in SPECT/CT data acquisition and figure preparation. This work was supported in part by the National Science Council, Taiwan (grants NSC 95-2314-B-303-005 and NSC 96-2321-B-303-001-MY2).

References

1. von Schulthess G. Introduction. In: von Schulthess G, ed. *Molecular Anatomic Imaging: PET-CT and SPECT-CT Integrated Modality Imaging*, 2nd ed. Philadelphia: Lippincott Williams & Wilkins, 2007:3–9.
2. Bocher M, Balan A, Krausz Y, et al. Gamma camera-mounted anatomical X-ray tomography: technology, system characteristics and first images. *Eur J Nucl Med* 2000;27:619–27.
3. O'Connor MK, Kemp BJ. Single photon emission computed tomography/computed tomography: basic instrumentation and innovations. *Semin Nucl Med* 2006;36:258–66.
4. Hasagawa BH, Stebler B, Rutt BK. A prototype high-purity germanium detector system with fast photon counting circuitry for medical imaging. *Med Phys* 1991;18:900–99.
5. Lang TF, Hasagawa BH, Liew SC, et al. Description of a prototype emission transmission computed tomography imaging system. *J Nucl Med* 1992;33:1881–7.
6. Kalki K, Blankespoor SC, Brown JK, et al. Myocardial perfusion imaging with a combined x-ray CT and SPECT system. *J Nucl Med* 1997;38:1535–40.
7. Tang HR, Da Silva AJ, Matthay KK, et al. Neuroblastoma imaging using a combined CT scanner—scintillation camera and ^{131}I-MIBG. *J Nucl Med* 2001;42:237–47.
8. King MA, Tsui BM, Pan TS, Glick SJ, Soares EJ. Attenuation compensation for cardiac single-photon emission computed tomographic imaging: part 2. Attenuation compensation algorithms. *J Nucl Cardiol* 1996;3:55–64.

9. Hutton BF, Hudson HM, Beekman FJ. A clinical perspective of accelerated statistical reconstruction. *Eur J Nucl Med* 1997;24:797–808.
10. Love C, Palestro CJ. Radionuclide imaging of infection. *J Nucl Med Technol* 2004;32:47–57.
11. De Winter F, Gemmel F, Van Laere K, et al. 99mTc-ciprofloxacin planar and tomographic imaging for the diagnosis of infection in the postoperative spine: experience in 48 patients. *Eur J Nucl Med Mol Imaging* 2004;31: 233–9.
12. Yapar Z, Kibar M, Yapar AF, Togrul E, Kayaselcuk U, Sarpel Y. The efficacy of technetium-99m ciprofloxacin (infection) imaging in suspected orthopaedic infection: a comparison with sequential bone/gallium imaging. *Eur J Nucl Med* 2001;28:822–30.
13. Bleeker-Rovers CP, Vos FJ, Wanten GJ, et al. 18F-FDG PET in detecting metastatic infectious disease. *J Nucl Med* 2005;46:2014–9.
14. Love C, Tomas MB, Tronco GG, Palestrol CJ. FDG PET of infection and inflammation. *Radiographics* 2005;25: 1357–68.
15. Hoffer P. Gallium: mechanisms. *J Nucl Med* 1980;21:282–5.
16. Newman RD, McAfee JG. Gallium-67 imaging in infection. In: Sandler MP, Coleman RE, Patton JA, eds. *Diagnostic Nuclear Medicine*, 4th ed. Philadelphia: Lippincott, Williams & Wilkins, 2004:1205–17.
17. Kao PF, Tsui KH, Leu HS, Tsai MF, Tzen KY. Diagnosis and treatment of pyogenic psoas abscess in diabetic patients: usefulness of computed tomography and gallium-67 scanning. *Urology* 2001;57:246–51.
18. Kao PF, Tzen KY, Tsui KH, Tsai MF, Yen TC. The specific gallium-67 scan uptake pattern in psoas abscesses. *Eur J Nucl Med* 1998;25:1442–7.
19. Kao PF, Chen KS, Tsai MF, Ng SH, Tzen KY. Repeated gallium-67 scan demonstrating an occult mycotic aneurysm of the aortic arch due to Salmonella. *Scand J Infect Dis* 2003;35:199–202.
20. Tzen KY, Yen TC, Yang RS, Lee CM, Kao PF, Lin KJ. The role of ^{67}Ga in the early detection of spinal epidural abscesses. *Nucl Med Commun* 2000;21:165–70.
21. Kao PF, Tzen KY, Tsai MF, Chen FP. Pyometra as a lower abdominal doughnut sign on a Ga-67 scan. *Clin Nucl Med* 2000;25:485–6.
22. Kao PF, Tzen KY, Tsai MF, Yang KJ. Gallium-67 scanning in endogenous *Klebsiella* endophthalmitis with unknown primary focus. *Scand J Infect Dis* 2000;32:326–8.
23. Swayne LC. Computer-assisted fusion of single-photon emission tomographic and computed tomographic images. Evaluation in complicated inflammatory disease. *Invest Radiol* 1992;27:78–83.
24. Bar-Shalom R, Yefremov N, Guralnik L, et al. SPECT/CT using ^{67}Ga and ^{111}In-labeled leukocyte scintigraphy for diagnosis of infection. *J Nucl Med* 2006;47:587–94.
25. Kao PF, Huang MJ, You DL, Tzen KY. Using ^{131}I MIBG and ^{99m}TC-MDP bone scan for localization of rare extra-adrenal pheochromocytomas: report of 2 cases. *J Formos Med Assoc* 1992;91(Suppl 4):S283–7.
26. Kao PF, Tzen KY, Huang MJ, You DL. Obstructive hydronephrosis with I-131 MIBG accumulation mimicking huge pheochromocytoma: a diagnosis pitfall found with Tc-99m MDP imaging. *Clin Nucl Med* 1996;21:994–5.
27. Kao PF, Chang HY, Tsai MF, Lin KJ, Tzen KY, Chang CN. Breast uptake of iodine-131 mimicking lung metastases in a thyroid cancer patient with a pituitary tumour. *Br J Radiol* 2001;74:378–81.
28. Leitha T, Staudenherz A. Frequency of diagnostic dilemmas in ^{131}I whole body scanning. *Nuklearmedizin* 2003;42: 55–62.
29. Krausz Y, Klein M, Uziely B, et al. Impact of SPECT/CT on assessment of I-131 avid sites in differentiated thyroid cancer. *J Nucl Med* 2004;45:349.
30. Ruf J, Lehmkuhl L, Bertram H, et al. Impact of SPECT and integrated low-dose CT after radioiodine therapy on the management of patients with thyroid carcinoma. *Nucl Med Commun* 2004;25:1177–82.
31. Tharp K, Israel O, Hausmann J, et al. Impact of ^{131}I-SPECT/CT images obtained with an integrated system in the follow-up of patients with thyroid carcinoma. *Eur J Nucl Med Mol Imaging* 2004;31:1435–42.
32. O'Doherty MJ, Kettle AG, Wells P, Collins RE, Coakley AJ. Parathyroid imaging with technetium 99m-sestamibe: preoperative localization and tissue uptake studies. *J Nucl Med* 1992;33:313–8.
33. Takebayashi S, Hidai H, Chiba T, Takaga Y, Nagatani Y, Matsubara S. Hyperfunctional parathyroid glands with ^{99m}TC-MIBI scan: semi-quantitative analysis correlated with histologic findings. *J Nucl Med* 1999;40:1792–7.
34. Ohshima A, Simizu S, Okido M, Shimada K, Kuroki S, Tanaka M. Endoscopic neck surgery: current status for thyroid and parathyroid diseases. *Biomed Pharmacother* 2002;56:48s–52s.
35. Medrano C, Hazelrigg SR, Landreneau RJ, Boley TM, Shawgo T, Grasch A. Thoracoscopic resection of ectopic parathyroid glands. *Ann Thorac Surg* 2000;69:221–3.
36. Denham DW, Norman J. Cost-effectiveness of preoperative sestamibi scan for primary hyperparathyroidism is dependent solely upon the surgeon's choice of operative procedure. *J Am Coll Surg* 1998;186:293–305.
37. Gotthardt M, Lohmann B, Behr TM, et al. Clinical value of parathyroid scintigraphy with technetium-99m methoxyisobutylisonitrile: discrepancies in clinical data and a systematic meta-analysis of the literature. *World J Surg* 2004;28:100–7.
38. Lumachi F, Ermani M, Basso S, Zucchetta P, Borsato N, Favia G. Localization of parathyroid tumors in the minimally invasive era: which technique should be chosen? Population-based analysis of 253 patients undergoing parathyroidectomy and factors affecting parathyroid gland detection. *Endocr Relat Cancer* 2001;8:63–9.
39. Lorberboym M, Minski I, Macadziob S, Nikolor G, Schachter P. Incremental diagnostic value of preoperative ^{99m}Tc-MIBI SPECT in patients with a parathyroid adenoma. *J Nucl Med* 2003;44:904–8.
40. Gayed IW, Kim EE, Broussard WF, et al. The value of ^{99m}Tc-sestamibi SPECT/CT over conventional SPECT in the evaluation of parathyroid adenomas or hyperplasia. *J Nucl Med* 2005;46:248–52.
41. Krausz Y, Bettman L, Guralnik L, et al. Technetium-99m-MIBI SPECT/CT in primary hyperparathyroidism. *World J Surg* 2006;30:76–83.
42. Schillaci O, Filippi L, Danieli R, Simonetti G. Single-photon emission computed tomography/computed tomography in abdominal diseases. *Semin Nucl Med* 2007;37:48–61.
43. Choi BY, Nguyen HM. The diagnosis and management of benign hepatic tumors. *J Clin Gastroenterol* 2005;39: 401–12.
44. Royal HD, Brown ML, Drum DE, Nagle CE, Sylvester JM, Ziessman HA. Procedure guideline for hepatic and splenic imaging. Society of Nuclear Medicine. *J Nucl Med* 1998; 39:1114–6.

45. Ziessman HA, Silverman PM, Patterson J, et al. Improved detection of small cavernous hemangiomas of the liver with high-resolution three-headed SPECT. *J Nucl Med* 1991;32:2086–91.
46. Birnbaum BA, Noz ME, Chapnick J, et al. Hepatic hemangiomas: diagnosis with fusion of MR, CT, and Tc-99m-labeled red blood cell SPECT images. *Radiology* 1991; 181:469–74.
47. Schillaci O, Danieli R, Manni C, Capoccetti F, Simonetti G. Technetium-99m-labelled red blood cell imaging in the diagnosis of hepatic hemangiomas: the role of SPECT/CT with a hybrid camera. *Eur J Nucl Med Mol Imaging* 2004; 31:1011–5.
48. Zheng JG, Yao ZM, Shu CY, Zhang Y, Zhang X. Role of SPECT/CT in diagnosis of hepatic hemangiomas. *World J Gastroenterol* 2005;11:5336–41.
49. Castellani M, Cappellini MD, Cappelletti M, et al. Tc-99m sulphur colloid scintigraphy in the assessment of residual splenic tissue after splenectomy. *Clin Radiol* 2001;56: 596–8.
50. Gunes I, Yilmazlar T, Sarikaya I, Akbunar T, Irgil C. Scintigraphic detection of splenosis: superiority of tomographic selective spleen scintigraphy. *Clin Radiol* 1994;49:115–7.
51. Horger M, Eschmann SM, Lengerke C, Claussen CD, Pfannenberg C, Bares R. Improved detection of splenosis in patients with haematological disorders: the role of combined transmission-emission tomography. *Eur J Nucl Med Mol Imaging* 2003;30:316–9.
52. Valdes Olmos RA, Horenblas S, Kartachova M, Hoefnagel CA, Sivro F, Baars PC. ^{99m}Tc-labelled heat-denatured erythrocyte SPECT-CT matching to differentiate accessory spleen from tumour recurrence. *Eur J Nucl Med Mol Imaging* 2004;31:150.
53. Howart DM. The role of nuclear medicine in the detection of acute gastrointestinal bleeding. *Semin Nucl Med* 2006; 36:133–46.
54. Yama N, Ezoe E, Kimura Y, et al. Localization of intestinal bleeding using a fusion of Tc-99m-labeled RBC SPECT and X-ray CT. *Clin Nucl Med* 2005;30:488–9.
55. Krag DN, Weaver DL, Alex JC, Fairbank JT. Surgical resection and radiolocalization of the sentinel lymph node in breast cancer using a gamma probe. *Surg Oncol* 1993;2: 335–40.
56. Liu SH, Chang WC, Kao PF, et al. Lymphoscintigraphy and intraoperative gamma probe-directed sentinel lymph node mapping in patients with malignant melanoma. *J Formos Med Assoc* 2004;103:41–6.
57. Chetty U, Jack W, Prescott RJ, Tyler C, Rodger A. Management of the axilla in operable breast cancer treated by breast conservation: a randomized clinical trial. Edinburgh Breast Unit. *Br J Surg* 2000;87:163–9.
58. Schrenk P, Rieger R, Shamiyeh A, Wayand W. Morbidity following sentinel lymph node biopsy versus axillary lymph node dissection for patients with breast carcinoma. *Cancer* 2000;88:608–14.
59. Husarik DB, Fehr M, Thuerl CM, et al. Sentinel lymph node scintigraphy in breast cancer: incremental value of SPECT/CT imaging. *J Nucl Med* 2005;46:197.
60. Husarik DB, Steinert HC. Single-photon emission computed tomography/computed tomography for sentinel node mapping in breast cancer. *Semin Nucl Med* 2007;37:29–33.
61. Lerman H, Metser U, Lievshitz G, Sperber F, Shneebaum S, Even-Sapir E. Lymphoscintigraphic sentinel node identification in patients with breast cancer: the role of SPECT/CT. *Eur J Nucl Med Mol Imaging* 2006;33:329–37.
62. van der Ploeg IMC, Valdes Olmos RA, Nieweg OE, Rutgers EJT, Kroon BBR, Hoefnagel CA. The additional value of SPECT/CT in lymphatic mapping in breast cancer and melanoma. *J Nucl Med* 2007;48:1756–60.
63. Huang JY, Kao PF, Chen YS. *Visual Enhancement for Sentinel Lymph Node Mapping in Breast Cancer by Multiple Display Formats of SPECT/CT Images.* The International Conference on Bio Medical Engineering and Informatics (BMEI2008), Hainan, China, 2008.
64. Kao PF, Huang JY, Chen YS. *SLN SPECT/CT 3D Display with Bone Co-registration.* The Society of Nuclear Medicine 55th Annual Meeting, New Orleans, Louisiana, USA, 2008.
65. Horger M, Bares R. The role of single-photon emission computed tomography/computed tomography in benign and malignant bone disease. *Semin Nucl Med* 2006;36:286–94.
66. Even-Sapir E. Imaging of malignant bone involvement by morphologic, scintigraphic, and hybrid modalities. *J Nucl Med* 2005;46:1356–67.
67. Kao PF, Tzen KY, Chen JY, Lin KJ, Tsai MF, Yen TC. Rectus abdominis rhabdomyolysis after sit ups: unexpected detection by bone scan. *Br J Sport Med* 1998;32:253–4.
68. Kao PF, Tzen KY, Chang LY, You DL, Yang JY. ^{99m}Tc-MDP scintigraphy in high-voltage electrical burn patients. *Nucl Med Commun* 1997;18:846–52.
69. Ergun EL, Kiratli PO, Gunay EC, Erbas B. A report on the incidence of intestinal ^{99m}Tc-methylene diphosphonate uptake of bone scans and a review of the literature. *Nucl Med Commun* 2006;27:877–85.
70. Loutfi I, Collier BD, Mohammed AM. Nonosseous abnormalities on bone scans. *J Nucl Med Technol* 2003;31:149–53.
71. Love C, Din AS, Tomas MB, Kalapparambath TP, Palestro CJ. Radionuclide bone imaging: an illustrative review. *Radiographics* 2003;23:341–58.